Title:
Design and Development of Longitudinal and Torsional Ultrasonic Vibration-assisted Needle Insertion Device for Medical Applications

Authors:
Yi Wang, ywang152@ncsu.edu, North Carolina State University, Raleigh, NC, U.S.A.
Yi Cai, ycai@ncat.edu, North Carolina Agricultural and Technical State University, U.S.A.
Yuan-Shin Lee*, yslee@ncsu.edu, North Carolina State University, Raleigh, NC, U.S.A.

Keywords:
Vibratory needle insertion, Biologically Inspired Design, Longitudinal-torsional vibration, Medical Applications, Finite Element Analysis

DOI: 10.14733/cadconfP.2021.277-282

Introduction:
This paper presents a new design of longitudinal and torsional (L&T) ultrasonic vibration device for accurate needle insertion in medical applications. Needle insertion as a critical medical procedure is widely conducted for biopsy, brachytherapy, drug delivery, injection therapy, neurosurgery, medical treatments, etc. [1]. It is important in medical treatments to place the needle to the treatment spots as accurately as possible. Inspired by insects in nature, a flexible and bendable tube could penetrate animal skins with vibration, hence vibration-assisted needle insertion with accuracy could possibly be achieved.

To improve needle insertion performance, vibration-assisted insertion as a dynamic insertion method has been researched and demonstrated useful. Currently, extensive research focuses on the effect of the axial vibration on the needle insertion, showing a vibratory needle can effectively reduce the friction force and cutting force, thereby reducing the insertion force. Huang et al. [6] indicated high-frequency vibration reduces 28% of the friction and cutting force in needle insertion. Barnett et al. [3], [8] reported the insertion force can be reduced by as much as 35% using 25 μm peak-peak oscillation. Unfortunately, it is difficult to achieve high-frequency large-amplitude ultrasonic vibration within a compact ultrasonic device due to the corresponding large mechanical impedance. While the insertion force is reduced by larger vibration amplitude and higher frequency, it has also been observed a larger area of tissue damage during the insertion [8]. To explore the potentials of vibratory needle insertion, the longitudinal vibration is extended to a three-dimensional vibration. In our earlier works presented in [4], [5], [7], a new design of longitudinal-flexing vibratory surgical needle was developed by adding a series of micro slots on the needle. The experimental results demonstrated that three-dimensional vibration can further reduce puncture force and friction than longitudinal vibratory needles..

In this paper, we present a new design of longitudinal and torsional (L&T) ultrasonic vibration device for accurate medical needle insertion in medical applications. A waveguide-based Langevin type L&T ultrasonic transducer is proposed and 3D printed for the vibration-assisted insertion device. The finite element model and analysis are conducted to study the vibration characteristics of the design. Laboratory experiments were carried out to validate the effectiveness of the new L&T vibration transducer design. The experiment results show the proposed new L&T vibratory needle insertion device is able to accurately deliver the needle to the target depth and location.

Design of the Vibration-assisted L&T Needle Insertion Device:
Fig. 1 shows a design of a waveguide-based Langevin type L&T ultrasonic vibration device for needle insertion. The Langevin type transducer can achieve high electromechanical conversion efficiency and

be only excited by the axial polarized PZT ceramic stacks with single ultrasonic driving power. Although some L&T ultrasonic transducers were developed earlier by modifying the exterior structures of the transducer by machining, the inner cylindrical part remains solid, making only the axial vibration dominating the combined vibration. Given such structure, it is difficult to correctly find the synchronous plane and the resonant frequency of both the longitudinal and the torsional vibration modes.

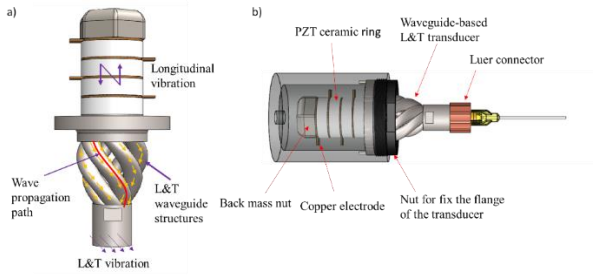

Fig. 1: Design of the L&T waveguide-based ultrasonic vibration device.

In our earlier work presented in [2], [7], [10], a waveguide structure can directly guide the wave propagation direction with high efficiency. In this paper, as shown in Fig. 1(a), a helical structure was proposed and used as the waveguide to alter the longitudinal wave propagation to achieve an L&T ultrasonic vibration. To achieve the desired wave propagation direction, the wave propagation path should be first defined. A helical path for the wave propagation path was designed and described as a circular helix in cylindrical coordinate, shown as follows:

$$\mathrm{P}(l) = \begin{cases} x(\theta) = \frac{d}{2}cos\theta \\ y(\theta) = \frac{d}{2}sin\theta, \ \theta\epsilon[0,\pi] \\ z = \frac{L}{2\pi}\theta \end{cases} \tag{1}$$

where d is the diameter of the circular helix, θ is the rotational angle, and L is the height of the helix. A circular array of six such helical paths was then designed to form a tapered shape when the rotational angle θ starts from 0 degrees and ends at 180 degrees. The tapered shape is able to combine and boost the synchronous vibration to achieve a harmonic L&T vibration at the front output end. As discussed in our earlier work [9], the resultant exertion forces F_{ext_end} and the resultant exertion moments M_{ext_end} from the six waveguides can be presented as follows (details presented in our earlier work [10]):

$$F_{ext_{end}} = \frac{\partial\left(\iiint \rho\frac{\partial\overrightarrow{u_M}}{\partial t}dV\right)}{\partial t} = \sum_{i=1}^{6} F_{ext_i} \tag{2}$$

$$M_{ext_{end}} = \frac{\partial\left(\iiint \rho\overrightarrow{GM}\times\frac{\partial\overrightarrow{u_M}}{\partial t}dV\right)}{\partial t} = \sum_{i=1}^{6} M_{ext_i} \tag{3}$$

where ρ is the mass density of the waveguide material, V is the corresponding volume, vectors are corresponding vibration displacements. To fit various types of commercial needles, a commercial Luer connector was adopted, as shown in Fig.1 (b). Base on the size of the Luer connector, the diameter of the front end of the transducer was determined as 10 mm. To minimize the size of the device and ensure the vibration amplitude, we employed four pieces of commercially available axial polarized Lead Zirconate Titanate (PZT-8) piezoelectric ceramic rings. The PZT-8 ceramic rings have an outer diameter of 15 mm and an inner diameter of 10 mm. They are compressed by a 1045 steel heavy back mass nut to transfer wave forward efficiently. Based on these critical sizes, the cross-section of each waveguide structure was designed as 4.5 mm in diameter. An aluminum shell was designed to seal the piezoelectric ceramics and fix the flange of the transducer. The CAD model was imported to finite analysis software ANSYS® 19.1 for vibration characteristics analysis, as discussed in the next section.

Finite Element Analysis of The New L&T Design:

To optimize the design of the L&T transducer, a harmonic response analysis was conducted for the steady-state vibration behavior of the proposed L&T vibration-assisted insertion device. The waveguide-based L&T transducer with a 20 mm long blunt needle was built in the FE model. The Piezo and MEMS module embedded in the ANSYS Workbench was adopted to simulate the exciting voltage applied to the piezoelectric ceramic rings. A fixed constrain boundary condition was added to the flange region of the transducer. Fig. 2 (a) shows the vibration amplitude response results versus the corresponding frequencies. It can be found that both the peaks of longitudinal and torsional vibrations have the same resonant frequency at 48.6 kHz. That means the longitudinal and torsional vibrations successfully resonate at the same time. At this resonant frequency, the amplitude of torsional vibration is slightly larger than that of longitudinal vibration. Fig. 2 (b) shows the vibration displacements at the resonant frequency. A steady-state synchronized L&T vibration occurs at the tip of the needle. Importantly, the maximum L&T deformation appears at the tip of the needle.

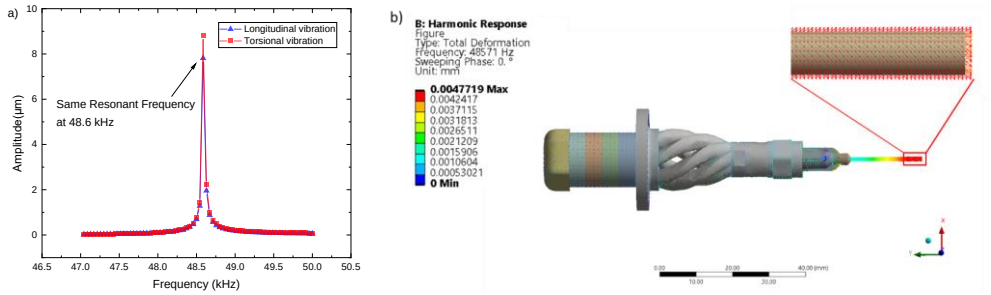

Fig. 2: Harmonic response simulation results: (a) vibration amplitudes versus sweeping frequencies, (b) vibration shape at the resonant frequency 48.6 kHz.

Fabrication and Assembly of the Device:

The prototype of the L&T ultrasonic vibration-assist needle insertion device was fabricated for laboratory experiments. Due to the complex geometric shape of the new transducer, the design was fabricated by using the selective laser melting (SLM) additive manufacturing (AM) process with AlSi10Mg metal powders, as shown in Fig. 3 (a) left-top. A finishing operation was then applied to machine threads and flange regions for assembly purposes. The Luer connector is assembled to the transducer using threads. To compare with the L&T vibration, a longitudinal vibration transducer was also designed and fabricated with the same critical dimensions, as shown in Fig. 3 (a) left-bottom. The same four pieces of PZT-8 ceramic rings were also used. To ensure the two transducers have a similar resonant frequency, the longitudinal vibration transducer was machined using Al 6061. The impedance analysis of these two transducers was also conducted, as shown in Fig. 3 (b). Both of them have a similar resonant frequency at around 49 kHz, which also has a good agreement with our FE analysis results of 48.6 kHz.

Experiments and Results on Needle Insertions:

Fig. 3 shows the experimental setup for the vibratory needle insertion system. A six-axis force sensor (ATI® gamma series) was used to measure the insertion force at the rate of 60 Hz. A 3D printed plastic fixture was installed on the force sensor to secure a beaker with Gelly® wax phantom tissue. A linear motor (FUYU® FLS40) was programmable controlled using a Raspberry Pi. The assembled vibratory insertion device was mounted on a linear guide. The PiezoDrive® PDUS210 driver was used to drive the ultrasonic device at its resonant frequency.

Fig. 4 (a) shows the insertion force measurement results at insertion speed of 0.5 mm/s under the following conditions: (1) no vibration, (2) longitudinal (L) vibration, (3) L&T vibration. Three identical insertion phases (pre-puncture, puncture, and post puncture) can be observed in Fig. 4 (a). Both the longitudinal vibration and L&T vibration are able to lower the puncture force by about 36% and 38%, respectively. In the post-puncture phase, the insertion force rapidly increased linearly.

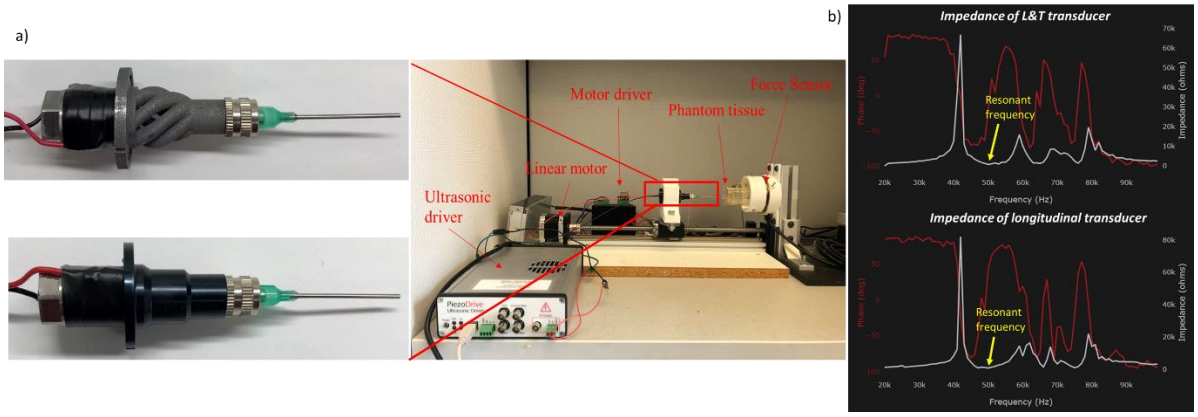

Fig. 3: Prototypes of L&T ultrasonic transducer and longitudinal transducer: (a) fabricated transducer and experiment setup, (b) corresponding impedance analysis results.

As shown in Fig. 4 (a), in this phase, L&T vibration reduces the maximum insertion force by 15%, compared with longitudinal vibration by 7%. The L&T vibration causes more insertion force reduction compared to the longitudinal-only vibration. To analysis the insertion force component, the friction force is the primary influencing factor in this phase, particularly as the needle penetrates deeper. In other words, L&T vibration could reduce more friction force, thereby lower the total axial insertion force.

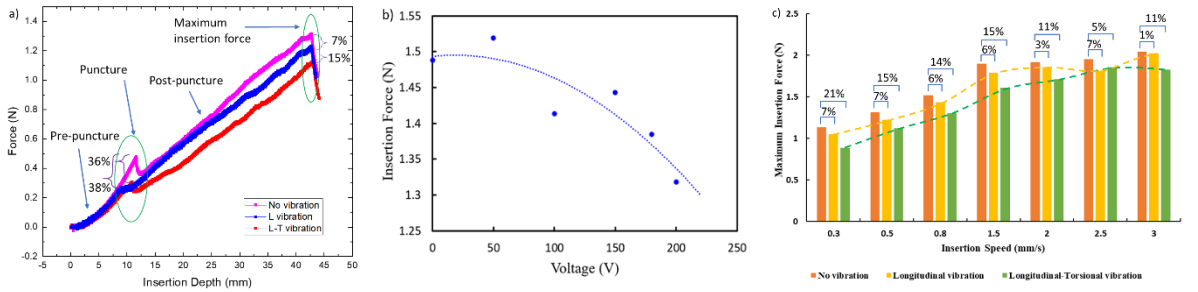

Fig. 4: Insertion experiment results: (a) an example of insertion force measurement, (b) insertion force vs. driving voltage, (c) maximum insertion force at different insertion speeds.

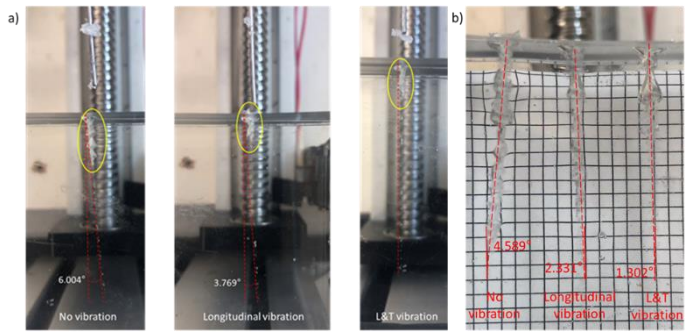

Fig. 5: Experiment shows the L&T insertion (the leftmost one) achieves the best accuracy.

To validate the effect, the relation between the insertion force reduction rate and resultant insertion speed was studied, as shown in Figs. 4 (b) and (c). The resultant needle insertion velocity vector $\vec{v}$ can be represented as Equation (4):

$$\vec{v} = \left(v_0 - A_L \omega cos(\omega t)\right)\overrightarrow{e_x} + A_T \omega cos(\omega t)\overrightarrow{e_y} \quad (4)$$

Where A_L and A_T are the longitudinal vibration amplitude and torsional vibration amplitude, respectively, and ω is the vibration frequency, $\overrightarrow{e_x}$ is the unit vector along insertion direction, and $\overrightarrow{e_y}$ is the unit vector perpendicular to the insertion direction. In the experiment, since the two types of transducers were designed with a similar resonant frequency, the superimposed vibration velocity can be changed by adjusting the driving voltage. Based on our earlier research in [10, 11], the waveguide-based L&T transducer has a good linear relation between the driving voltage and vibration amplitudes. In Fig 4 (b), we fixed the insertion speed at 1mm/s and only changed the vibration velocity by adjusting the driving voltage. It can be found that the insertion force decreases with increasing driving power. In Fig. 4(c), L&T vibration causes a lower insertion force, while the force reduction decrease with the increase of insertion speed. Fig. 5 shows comparation experiments using the developed L&T vibration transducer to insert thin and soft solder wire into phantom tissues for experimental bending observation. As shown in Fig. 5, the developed L&T vibration insertion is able to more accurately reach the targeted insertion location and depth than longitudinal only vibration and no vibration.

Conclusions:

In this paper, a new wave-guided L&T vibration-assisted needle insertion device was presented for medical applications. Analytical modeling of the waveguide L&T ultrasonic device was discussed. Both the simulation and the laboratory experiments have demonstrated the new 3D printed waveguide-based L&T transducer can deliver synchronized longitudinal and torsional vibrations at the same resonant frequency. The comparison confirms that the presented waveguide-based L&T insertion device is able to deliver much better insertion performance and higher insertion accuracy. The presented waveguide-based L&T ultrasonic vibration-assisted device can be possibly used for various types of medical treatment applications.

Acknowledgments:

The paper was partially supported by the National Science Foundation under Grant NSF-1938533 to NC State University as a sub-recipient. Their supports are greatly appreciated.

References:

[1] Abolhassani, N.; Patel, R.; Moallem, M.: Needle insertion into soft tissue: A survey, Medical Engineering & Physics, 29(4), 2007, 413–431. https://doi.org/10.1016/j.medengphy.2006.07.003.

[2] Al-Budairi, H.; Lucas M.; Harkness P.: A design approach for longitudinal–torsional ultrasonic transducers, Sensors and Actuators A: Physical, 198, 2013, 99–106. https://doi.org/10.1016/j.sna.2013.04.024.

[3] Barnett, A. C.; Wolkowicz, K.; Moore, J. Z.: Vibrating Needle Cutting Force, V002T02A025, Volume 2: Processing, Detroit, Michigan, USA, 2014. https://doi.org/10.1115/MSEC2014-4049.

[4] Cai, Y.; Moore, J.; Lee, Y.-S.: Novel surgical needle design and manufacturing for vibratory-assisted insertion in medical applications, Computer-Aided Design and Applications, 14(6), 2017, 833–843. https://doi.org/10.1080/16864360.2017.1287759.

[5] Cai, Y.; Moore, J.; Lee, Y.-S.: Vibration Study of Novel Compliant Needle used for Vibration-assisted Needle Insertion, CAD&A, 16(4), 2018, 742–754. https://doi.org/10.14733/cadaps.2019.742-754.

[6] Huang, Y. C.; Tsai, M. C.; Lin, C. H.: A piezoelectric vibration-based syringe for reducing insertion force, IOP Conference Series: Materials Science and Engineering, 42, 2012, 012020. https://doi.org/10.1088/1757-899X/42/1/012020.

[7] Ni, H.; Wang, Y.; Gong, H.; Pan, L.; Li Z. J.; D. Wang.: A novel free-form transducer for the ultra-precision diamond cutting of die steel, Int J Adv Manuf Technol, 95, 5–8, 2018, 2185–2192. https://doi.org/10.1007/s00170-017-1347-1.

[8] Tan, L.; Jones, J. A.; Barnett A. C.; Zhang H.; Moore J. Zhang Z.; Q.: Force Model for Ultrasonic Needle Insertion, Experimental Techniques, 42(5), 2018, 499–508. https://doi.org/10.1007/s40799-018-0255-0.

[9] Wang, Y.; Han, C.; Mei, D.; Xu, C.: Localized Microstructures Fabrication Through Standing Surface Acoustic Wave and User-Defined Waveguides, Volume 1: Additive Manufacturing; Manufacturing Equipment and Systems; Bio and Sustainable Manufacturing, Erie, Pennsylvania, USA, 2019, V001T05A005. https://doi.org/10.1115/MSEC2019-2879.

[10] Wang, Y.; Lee, Y.-S.; Y. Cai; Sun Y.; Gong H.: Design of Ultrasonic Longitudinal-Torsional Vibrator Based on Waveguide Principle for Manufacturing and Medical Applications, Procedia Manufacturing, 48, 2020, 114–122. https://doi.org/10.1016/j.promfg.2020.05.027.

[11] Wang, Y.; Shih, Y.-Y.; Lee, Y.-S: Vibration-assisted Insertion of Flexible Cortical Neural Microelectrodes with Bio-dissolvable Guides for Medical Implantation, 2021 ASME International Manufacturing Science and Engineering Conference. https://doi.org/10.1115/MSEC2020-1965.